Energy 270 (2023) 126885

Contents lists available at ScienceDirect

Energy

journal homepage: www.elsevier.com/locate/energy

Evaluating energy flexibility requirements for high shares of variable renewable energy: A heuristic approach

Natasa Vulic *, Martin Rüdisüli, Kristina Orehounig

Laboratory for Urban Energy Systems, Empa Dübendorf, Switzerland

ARTICLE INFO

Keywords:
Energy flexibility
Distributed generation
Variable generation
Solar PV
Energy supply/demand analysis

ABSTRACT

Efforts to reduce carbon intensity of electricity involve increasing shares of variable renewable energy (VRE), including a trend towards decentralized generation. Ensuring their high utilization necessitates addressing generation variability at different spatial and temporal scales, likely involving a coordination of multiple systems (e.g. flexible loads, storage, dispatchable generation). This paper presents a methodology for estimating the energy flexibility required from such a synchronized system. The simple data-based approach uses local load and VRE production patterns, and provides a regional assessment considering (1) indicators to evaluate energy flexibility requirements based on VRE self-consumption (2) visualization methods to observe consumption and production patterns' impact on flexibility requirements across day/week/year and (3) simple algorithms to estimate the energy flexibility requirements at different timescales. The approach is demonstrated for three Swiss distribution system operators, for both current and increased shares of VRE generation. The largest benefits for optimal self-consumption are realized for the energy flexibility timescale of 6–12 hrs. Medium- and long-term (seasonal) storage appears beneficial at VRE penetration levels beyond 40%. The proposed framework can be readily utilized to assess energy flexibility requirements of different regions, and serve as a basis for identifying a suitable mix of strategies needed to address them.

1. Introduction

1.1. Motivation

National energy systems are facing a major challenge: reducing greenhouse gas (GHG) emissions while providing equitable and secure access to electricity [1]. Addressing this challenge has centered on increasing shares of variable renewable energy (VRE), with solar and wind now meeting an appreciable share of global electricity demand (approx 8% in 2019 [2]), while also accounting for the majority of the newly installed capacity [3]. Distributed solar photovoltaic (PV) installations by private households and small-to-medium sized businesses contributed to approx. 20% of the global renewable capacity in 2019 [4].

VRE generation varies at different timescales governed by atmospheric conditions—from the less predictable short-term variations to the more distinct daily and seasonal patterns. Optimized VRE utilization therefore depends upon available flexibility choices at different timescales. Various solutions could play a role in addressing this need, including flexible generation technologies, flexible demand [5–8], short- to medium-term storage (hours to weeks), sector-coupling (Power-to-Heat [9], Vehicle-to-Grid [10]) and long-term storage (Power-to-X [11]). Additional market-based strategies that incentivize small end-consumers and producers to become active participants in the electricity market (e.g. virtual power plants [12], flexibility trading platforms [13]) may also be needed. However, given a wide range of timescales for the required flexibility, no single solution is likely to meet them all. Rather, it would require a combination of multiple energy systems acting in a coordinated way, able to respond to system needs by storing and releasing electricity [14]. Quantifying the energy flexibility requirements for this virtual energy storage system (VESS) can serve to identify the appropriate mix of technological and market-based solutions needed to address them.

Flexibility requirements between different regions are expected to vary, with demand patterns, VRE type and penetration, as well as grid inter-connectivity playing an important role. In order to identify them, and compare them side-by-side, as well as estimate how they are expected to evolve, requires a heuristic approach. Increased VRE generation, especially in the distribution grid, poses added challenges for the distribution system operators (DSOs) to plan for and manage distributed energy resources (DER) – local generation, flexible loads and storage – while reducing network expansion investment [15,16].

* Corresponding author.
E-mail address: natasa.vulic@empa.ch (N. Vulic).

https://doi.org/10.1016/j.energy.2023.126885
Received 12 November 2021; Received in revised form 31 January 2023; Accepted 5 February 2023
Available online 7 February 2023

Glossary

DER	Distributed energy resources
DHW	Domestic hot water
DSO	Distribution system operator
GHG	Green house gas
HV	High voltage
LV	Low voltage
MV	Medium voltage
PV	Photovoltaic
SFH	Single family home
SH	Space heating
TS	Transformer station
$VESS$	Virtual energy storage system
VRE	Variable renewable energy

At the same time, DSOs exhibit great diversity in terms of size, network levels they operate (low, medium, and sometimes high voltage), end-consumers they serve (residential, commercial, industrial), climate conditions, end-use electrification (e.g. heating/cooling, mobility), grid structure, VRE penetration level, as well as access to DERs [17–19].

Based on available literature on how to estimate flexibility needs at the local scale (see next section), this paper proposes novel flexibility indicators based on *spatially-aware* VRE utilization that can be used for side-by-side comparison between different DSOs, as well as to monitor their progress towards increased self-sufficiency. Addressing VRE self-sufficiency at this level becomes especially important for regions where national VRE mandates are largely expected to be met through decentralized generation. Additionally, we include a simple algorithm to estimate how their energy flexibility requirements are expected to evolve with increased VRE generation, independent of technology/strategy that may be used to supply this energy flexibility.

1.2. Literature review

The effects of VRE generation on power and energy systems have been previously studied using both power flow and time-series analysis. Using detailed network models, the former explores physical effects of variability on grid operation (e.g. over-voltage, congestion, etc. [20,21]) that impact the quality and security of supplied electricity. As the European DSO Observatory study demonstrates, diversity in grid structures between DSOs requires detailed data to build representative network models for each region [17,19], which is needed to evaluate the impact of different VRE integration strategies on the grid [22]. To reduce the need for a detailed grid representation, the concept of electrical hubs has also been used to evaluate operational flexibility in distributed energy systems [23]. On the other hand, time-series analyses usually use a combination of historical data and VRE projections [24], which can be applied to balancing areas of different scales and over longer time-frames (e.g. months to years). Several studies have used time-series analyses to evaluate a system's need for flexibility across a number of locations (Germany [25], Ireland [26], France [27], Texas [28], Denmark [29], as well as multiple regions [30]), which consider either PV or wind or a combination of the two. Holttinen et al. [30] used it to identify the impact of large wind penetration on ramp magnitude and occurrence patterns (e.g. diurnal/monthly). Similarly, Lannoye et al. [26] take the time-series of changes in net load as a system's requirement for flexibility (and quantifies it for different time horizons) to identify when a power system cannot cope with these changes. On the other hand, Ueckerdt et al. [25] use residual load duration curves to analyze the impact of VRE on long-term generation capacity planning. These studies consider the evolving *power* flexibility requirements with increased VRE generation. In another study, Denholm and Mai [28] explore the *energy* flexibility requirements, specifically energy storage duration needed to reduce VRE curtailment under high-VRE scenarios (including the impact of a wind/PV generation mix) using a chronological dispatch of aggregated conventional units and energy storage with the NREL's REFlex model [31]. Heggarty et al. [27] provide a more general (technology-independent) approach to quantifying energy flexibility requirements at different timescales (annual, weekly, daily) using frequency analysis, including the impact of different factors (degree of network interconnection, VRE penetration mix, and electrified heating/cooling). Both of the above studies demonstrate the impact that diurnal/seasonal cycles of VRE production and end-consumption have on the timescales of energy flexibility requirements (from hourly to annual), which can be utilized for providing general guidelines for planning of VESS. While VRE penetration, as well as the VRE generation mix, are identified as primary determinants of energy flexibility requirements, the latter study also shows the impact that seasonal demand variations (due to electrified heating and cooling) have on the annual energy flexibility requirements. Olsen et al. [29] use a similar frequency method, and present the time-resolved energy flexibility requirements in an intuitive way for the case of the goal VRE penetration in Denmark. Both Heggarty et al. and Olsen et al. also show that increased VRE penetration has a greater effect on the *energy* flexibility capacity requirement than the *power* flexibility capacity requirement.

1.3. Original contribution and manuscript structure

The literature already provides evidence that increased VRE production raises energy flexibility requirements at different timescales, which are affected by the VRE penetration level (and its generation mix), as well as seasonal demand. Consequently, with increased distributed generation, different regions will likely experience unique energy flexibility needs, requiring separate models. Nevertheless, most time-series models are applied at the highest (transmission system operator) network level, and do not consider the impact of regional differences. On the other hand, studies featuring higher spatial resolution often resort to complex models requiring a high degree of detail about the energy system. As a result, they cannot be readily applied on a wider scale to allow comparison of different regions side-by-side and/or to track their progress over time; both are needed in order to provide a basis for choosing a regionally-specific mix of strategies able to meet their energy flexibility requirements.

The main objective of this study is to develop practical ways to examine typical available data from DSOs and define a simple approach to estimate region's energy flexibility needs based on them. Prior to extensive digitization, analysis of aggregated data at the local (DSO) level can help identify when and (to a certain extent) where, energy flexibility is most needed—both now and in the future. We define simple indicators to characterize the performance of an energy system based on VRE utilization, while also being able to identify the presence of spatial mismatch within a system boundary (between local demand and VRE production) using only their aggregated time-series profiles. Additionally, a simple algorithm for estimating temporally-resolved energy flexibility requirements, which are not technology-dependent, is provided. As proof-of-concept, we demonstrate the proposed methodology for three small- to medium-sized DSOs in Switzerland, a country that currently meets 4.5% of its demand through PV generation [32], primarily from smaller systems in the distribution grid [33]. The VRE mandates primarily focus on increasing PV generation (40% of total production by 2050) accompanied by the phase out of nuclear, with the remainder covered mainly by hydroelectricity (53%) [34]. Significant differences between the DSOs – in structure, size, and VRE implemen-

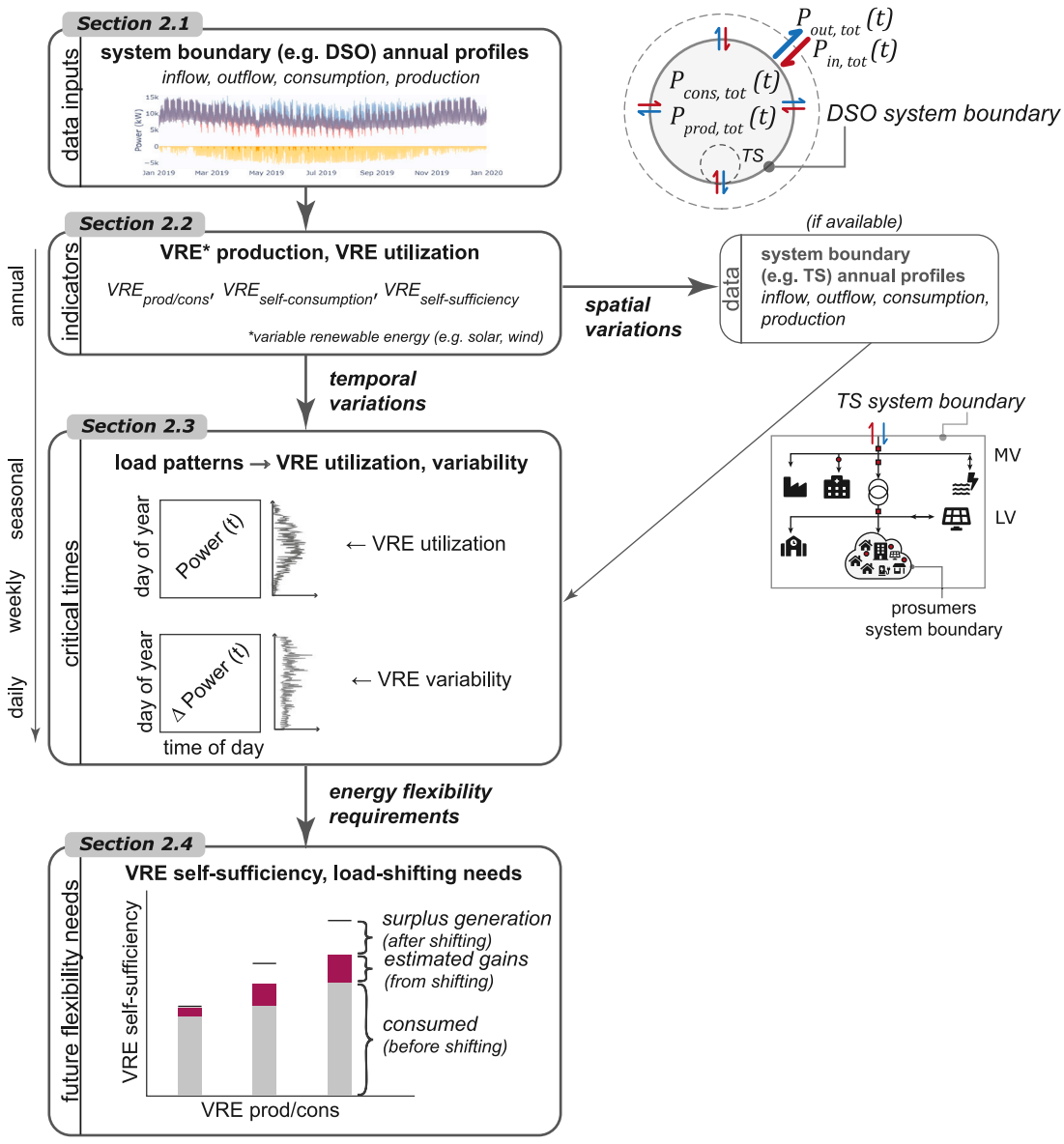

Fig. 1. General overview of the proposed methodology.

tation – highlight the need for localized approaches to assess their current state and monitor their progress. Additionally, with most of the growth expected to take place in the distribution networks, due to the network constraints at this level, addressing VRE utilization at this scale is of high importance. At the same time, it necessitates a simple approach—with over 600 DSOs in Switzerland, separately modeling each one would be challenging. The method can provide a basis for relevant stakeholders to evaluate potential technology and market-based solutions most suitable for a particular area.

This paper is structured as follows. Section 2 presents the case studies and the methodology, including indicators and visualization methods used to identify critical times – when the generated electricity is either underutilized or variability is high – as well as estimate corresponding energy flexibility requirements. Section 3 shows the results of the case studies, including the impact of daily and seasonal load patterns on VRE utilization and energy flexibility requirements throughout the year (both current and future). Furthermore, limitations of the proposed methodology and an outlook for further study are briefly discussed. Section 4 summarizes the main findings.

2. Methods

The data-centered framework presented in this paper allows for evaluating flexibility needs of various DSOs using indicators, visualization techniques, and simplified algorithms to estimate energy flexibility requirements aimed at improving VRE utilization. A general overview of the proposed methodology is shown in Fig. 1. DSO system boundary measured profiles – electricity inflow, outflow, consumption, and production – form the basis of the presented analysis, and can therefore be applied to any DSO. We first adapt previously used indicators related to PV utilization (often applied at the building level) in Section 2.2. Then, we expand upon previous visualization techniques to observe daily, weekly, and seasonal patterns of PV generation and total demand, which, in combination with the indicators, serve to identify critical times as detailed in Section 2.3. To estimate the intra-daily energy flexibility requirements for improving VRE utilization at this scale, we present an accounting-based approach to balance production surpluses and deficits for various time windows (3–24 hrs) in Section 2.4. This methodology is demonstrated for three DSOs in Switzerland described

Table 1
Case study data (year 2019 profiles with 15-min resolution).

	Background information		Annual profiles[a]			Grid levels[b]	Electricity generation
	Population	Settlement	In/out	Prod.	Cons.		
DSO A[c]	6k	peri-urban	×	×	×	4–7	PV
↳Transformer (20 SFH)			×			4	PV
↳Prosumers (5 SFH)				×	×	7	PV
DSO B	16k	urban	×	×		4–7	PV
DSO C	35k	urban	×	×	×	2–7	hydro, PV

[a]In/out → system boundary electricity inflow/outflow; prod.→ production; cons.→ consumption.
[b]7 → low voltage (LV); 5 → medium voltage (MV); 3 → high voltage (HV); 6, 4, 2 → transformer levels [37].
[c]Operates grid levels 6–7.

in Section 2.1. In the following sections, these case studies and methods are described in more detail.

2.1. Data

In the following analysis, three sets of data are used: two from individual utilities (DSO A and B), with PV as their main source of production, and one for a utility with significant hydroelectric generation (DSO C). The three DSOs supply electricity to medium-sized towns in the cantons of Bern, Aargau, and Valais in Switzerland (from a total of 600+ DSOs serving a population of 8.6 million [18,35]). Due to confidentiality terms, the exact locations and specifications cannot be given (however, this does not affect the methods and results presented here). The various profiles are provided for the year 2019 at 15 min resolution. For DSO A only, subset profiles for one of its transformer stations (serving a residential neighborhood of 20 single family homes [SFH]), as well as a group of five downstream prosumers, are also included. Table 1 summarizes these data and includes corresponding supplementary information. The annual profiles available from the DSOs are indicated with ×; the missing profiles are derived from these. All of the indicated profiles in Table 1 are *aggregated*. The data from the DSOs was provided as part of the aliunid project [36].

Grid levels are indicated for each of the profiles. It is important to note that while data for DSO A is provided for grid levels 4–7, DSO A only operates levels 6–7. Therefore, each DSO is distinct in their degree of vertical integration, with DSO A operating the lowest grid levels and DSO C being the most vertically integrated (comprising low voltage [LV] to high voltage [HV] grids). Additional data, such as load control schedules for space heating (SH) and domestic hot water (DHW) systems (available for DSO B), complement the profiles by helping identify the sources of certain daily periodic and/or seasonal patterns. In addition, when DSOs have other generation sources within their system boundaries (aside from PV production), as is the case for DSO C, separate production profiles are provided. No grid energy storage is reported for the DSOs (aside from dammed hydroelectricity in DSO C). In addition, within each DSO boundary, the interconnection between the consumers can be either physical (i.e. grid) or market-related.

Eq. (1) for the net electricity flow at the system boundary (i.e. the net load) $P_{net}\ (t)$ captures the relationship between different types of annual profiles (indicated in Table 1) at each timestep t. Specifically, the expression relates the following annual profiles (i.e. timeseries data over a full year period) – inflow $P_{in,\,tot}(t)$ and outflow $P_{out,\,tot}(t)$ across the system boundary to the consumption $P_{cons,\,tot}(t)$ and production $P_{prod,\,tot}(t)$ within the boundary – as schematically represented in Fig. 1 (DSO system boundary inset).

$$P_{net}\ (t) = P_{in,\,tot}(t) + P_{out,\,tot}(t) = P_{cons,\,tot}(t) + P_{prod,\,tot}(t) \tag{1}$$

By convention, inflow and consumption profiles have positive values and outflow and production have negative values. This relationship is used to estimate missing profiles (e.g. net electricity flow, consumption). All calculations are performed on *aggregated* time-series profiles for the system boundaries indicated in Table 1. Any activation of energy flexibility of the VESS would be reflected as either an increase/decrease in the consumption/production terms.

Due to increased digitization, a DSO may already have additional data within their service area that allow a closer examination (e.g. transformer stations, individual end-consumer production/consumption) as is the case for DSO A. If available, similar analysis can be applied to subsets of the DSO as schematically shown for the transformer station (TS) system boundary (see Fig. 1 inset).

2.2. Definition of indicators to evaluate energy flexibility needs

To evaluate flexibility needs of DSOs, we adapt previously used indicators related to PV utilization, often applied at the building level (as described in Ref. [38]). Specifically, we relate the following two indicators: (1) portion of VRE production to total demand (not all of which is utilized within the system boundary) and (2) portion of total demand which is met with VRE generation. If all of the produced VRE electricity is used within the system boundary to meet the demand (i.e. ideal self-consumption), the two indicators would be equal. The first indicator ($\%VRE_{prod/cons}$) is defined in Eq. (2) below

$$\%VRE_{prod/cons} = \frac{\sum_1^T P_{prod,VRE}(t)}{\sum_1^T P_{cons,tot}(t)} * 100, \tag{2}$$

where $P_{prod,VRE}(t)$ is the VRE production profile and T is the number of timesteps. While the relative volume of VRE production to total consumption within a system boundary is a good initial indicator of region's flexibility needs, different DSOs with similar fractions of VRE production can still substantially differ in their ability to consume that electricity within their network area. This may be due to missing connections between areas with high production and high consumption, as well as temporal mismatch between production and consumption of the full network area. An important indicator of the network's flexibility needs is thus the portion of PV production which is self-consumed within its boundary, as defined in Eq. (3) below

$$VRE_{self\text{-}consumption} = \left(1 - \frac{\sum_1^T P_{out,VRE}(t)}{\sum_1^T P_{prod,VRE}(t)}\right), \tag{3}$$

where $P_{out,VRE}(t)$ is the excess VRE production. In the case when excess VRE production is the main contributor to the network outflows, then $P_{out,VRE} = P_{out,tot}$. For the DSOs A and B investigated here, where most of the production within the network area comes from PV, this is a valid assumption. In the case of intentional export from dispatchable plants (e.g. hydro production), as is the case for DSO C, $P_{out,VRE}$ can be estimated by comparing network outflows to the generation patterns of VRE and non-VRE sources.

The resulting self-sufficiency (i.e. percentage of total consumption met with VRE electricity produced within the boundary) is represented in Eq. (4) below:

$$\%VRE_{self\text{-}sufficiency} = \%VRE_{prod/cons} * VRE_{self\text{-}consumption}. \tag{4}$$

The presented VRE production and VRE self-sufficiency indicators are used to determine and compare VRE utilization of DSO balancing

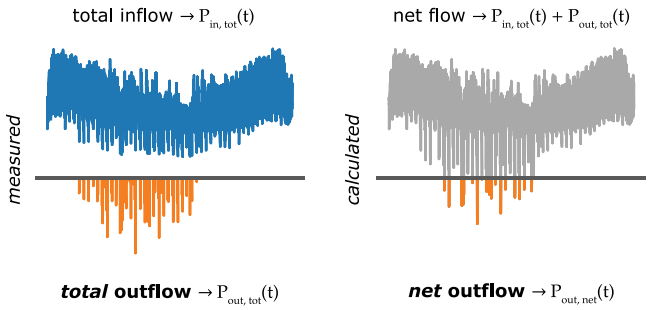

Fig. 2. Schematic representation of the actual (measured) and net outflow.

areas at different time scales (daily, annual) and spatial resolutions (e.g. TS, group of prosumers). If energy flexibility can be accessed to reduce surplus VRE production (e.g. by storing it for later use and/or shifting demand to uptake the surplus), both VRE self-consumption and self-sufficiency can be further increased.

As previously mentioned, the excess VRE production of a particular region can arise from either temporal or spatial mismatch, or a combination of the two. In order to separate the two contributions, we compare the results using the calculated net outflow ($P_{out,net}$) to the actual (measured) outflow ($P_{out,tot}$) of the network area. If only a single connection point exists between the network area and its super-ordinate grid, the two values are, by default, equal ($P_{out,net}(t) = P_{out,tot}(t)$). However, when inflows and outflows occur simultaneously at different connection points (i.e. $P_{in,tot}(t)$ and $P_{out,tot}(t)$ are both non-zero at timestep t), the net outflow is smaller than the measured, as schematically presented in Fig. 2. Eq. (5) shows the corresponding mathematical expression for calculating the net outflow:

$$P_{out,\,net}(t) = \begin{cases} P_{net}(t), & \text{if } P_{net}(t) \le 0 \\ 0, & \text{if } P_{net}(t) > 0 \end{cases} \tag{5}$$

By comparing the net to the actual outflow – in this case, surplus VRE production – the following interpretations can be made:

- If *net* surplus VRE production ≈ *actual* surplus VRE production (i.e. $P_{out,net} \approx P_{out,tot}$) and both values are non-negligible, the mismatch between consumption and production within the system boundary is mainly temporal
- If *net* surplus VRE production < *actual* surplus VRE production (i.e. $P_{out,net} < P_{out,tot}$), there is an additional spatial mismatch, with the degree of that mismatch indicated by the difference between these two values

2.3. Visualizing consumption and production patterns across day/week/year

To examine the patterns of electricity use and generation that impact VRE utilization, various time series profiles (e.g. consumption, production, net electricity flow) are represented as heatmaps. Their magnitudes are plotted along two dimensions – time-of-day and day-of-year – showing how daily profiles vary across week and season (similar to the method presented in Ref. [39]). The heatmaps are combined with daily VRE utilization indicators (from Section 2.2) in order to identify current (or anticipated) critical times related to surplus VRE production.

Similarly, changes in load (i.e. load ramps) are visualized alongside indicators of load variability. Specifically, the change in load (ΔP) from the previous to the current timestep (t), as expressed in Eq. (6) below, is computed for different time series profiles.

$$\Delta P(t+1) = P(t+1) - P(t) \tag{6}$$

The resulting ΔP profiles are then represented as heatmaps. A similar method was applied in Ref. [30] to visualize net load ramps with increased wind penetration. As an indicator of the observed load variability, a root mean square deviation (RMSD) from a nominal (zero-change) value is computed for each day of the year using Eq. (7) below

$$RMSD_{\Delta P} = \sqrt{\frac{\sum_1^T (0 - \Delta P(t))^2}{T}}, \tag{7}$$

where T is the number of timesteps. This helps to identify potential critical times related to high variability of VRE generation.

In addition to the heatmaps, average daily consumption and production profiles are calculated for four months representative of different seasons (January, April, July, and October), with consumption profiles also separated between weekdays and weekends. These profiles are compared to each other – within and across seasons – with regards to their shapes and relative magnitudes.

2.4. Estimating the maximum potential of activating intra-daily energy flexibility

Here we examine the impacts of increased VRE production on changing energy flexibility requirements at different timescales. The maximum benefit that a VESS meeting those requirements could provide (in terms of increased self-consumption) is then evaluated. In the analysis, we make the following simplified assumptions for each balancing group (e.g. DSO area):

- The annual consumption profile remains unchanged for higher VRE penetration scenarios (i.e. consumption profile for the year 2019 is used in all scenarios)
- The annual VRE production profile is scaled from the provided measured profile (i.e. VRE production profile is a scaled measured profile for the year 2019)
- Impact of network topology is not considered when evaluating surplus VRE production (taken as the net outflow in Eq. (5)) and the corresponding self-consumption (Eq. (3), where $P_{out,VRE}(t) = P_{out,net}(t)$)[1]
- Energy flexibility requirements are estimated for an ideal VESS (i.e no storage or transmission losses)

Measured VRE production profiles (in this case, PV) are scaled to specific annual production levels – from 20 to 100% of annual demand – where 100% $P_{prod/cons}$ indicates a net zero case (i.e. equal levels of production and consumption within a one year period). For each of these production levels, $VRE_{self\text{-}sufficiency}$ (Eq. (4)) is first computed for the base (no load-shifting) case. Then, load-shifting windows of various duration (between 3 and 24 hrs) are applied over the course of the year, and the maximum benefit of this load shift is computed. More specifically, for an nth day, the netflows are balanced for each load-shifting window (w) (balancing out potential inflows and outflows that occur within the ith time window) and the new net outflow $P_{out,n}$ computed for each day of the year (as shown in the Eq. (8) below).

$$P_{out,n} = \sum_{i=0}^{i=24/w} P_{net,n,i}(t)\Delta t[P_{net,n,i}(t) < 0] \tag{8}$$

The expression $[P_{net,n,i}(t) < 0]$ is an indicator function, which evaluates to 1 if True and 0 if False, ensuring that only surpluses are considered (similar to Eq. (5)). The corresponding net load within the ith time window ($P_{net,n,i}$) is shown in the Eq. (9) below:

$$P_{net,n,i} = \sum_{j=i}^{j=i+w} P_{net,j}(t)\Delta t. \tag{9}$$

[1] To determine the actual outflow with increased VRE production, detailed network topology with specific spatial distribution of simulated profiles is needed.

Table 2
Flexibility needs comparison (annual).

	$\%PV_{prod/cons}$	$\%PV_{self\text{-}sufficiency}$	
		Net	Actual
DSO A	11.9	11.9	7.6
↳Transformer	10.2	7.0	7.0
↳Prosumers	180	21	14
DSO B	8.7	8.7	8.5
DSO C	3.8	3.8	3.8

The resulting net outflows, computed over the course of the year, are then used to determine the corresponding daily and annual VRE self-sufficiency for each of the specified VRE production levels.

3. Results and discussion

3.1. Energy flexibility needs comparison with respect to spatial and temporal mismatch

The following analysis gives an overall indication of flexibility needs related to the utilization of VRE electricity (in this case PV) over the course of the year, enabling a quick side-by-side comparison of different DSOs. In Table 2, we compare the three DSOs based on their annual PV production levels ($VRE_{prod/cons}$ from Eq. (2)), as well as the corresponding self-sufficiency values ($VRE_{self\text{-}sufficiency}$ from Eq. (4)) that take into account their surplus production (both net and actual, as defined in Fig. 2). For DSO A, data for one of the transformer stations (connected to the superordinate grid), as well as a group of five prosumers downstream of the transformer, are also included; they illustrate how localized temporal mismatch between production and consumption contributes to the spatial mismatch observed for the full balancing area.

When we compare the three DSOs using these indicators, with respect to the type and degree of mismatch (between production and consumption), we observe large differences among them. The first two DSOs have comparable PV production levels as portion of their total consumption, 8.7 and 11.9%, respectively. Nevertheless, after PV production surpluses are taken into account, the resulting PV self-sufficiency drops only slightly for DSO B (to 8.5%), but quite substantially for DSO A (to 7.6%). While their *net* production surpluses reveal negligible temporal discrepancies for their respective network areas (negligible for DSO A, non-existent for DSO B), their *actual* production surpluses reveal considerable differences in terms of spatial mismatch: 36% and 1.7% of their PV production for DSOs A and B, respectively. In other words, while DSO B currently has a good match between PV production and consumption in terms of location – due to either (1) PV systems being located in areas with high consumption and/or (2) network area being well-connected and able to displace localized surpluses within the network boundary – DSO A appears less able to effectively utilize its localized PV production surpluses. When considering their respective characteristics in terms of PV system location (NE 7 vs. NE 5, 7) and distribution system operation (NE 6–7 vs. NE 4–7) it becomes clear why DSO A currently has both a greater need and a challenge displacing their localized PV production surpluses to other areas within their network boundary—localized PV production surpluses are both more likely, and these surpluses also directly outflow to the superordinate DSO (outside of their network boundary). Upon closer examination of one of the transformer stations in DSO A, we observe that PV self-sufficiency is consistent with that of the full network area (7.0% vs. 7.6%). In addition, downstream of this transformer station, further spatial mismatch is evidenced by the high production to consumption ratio of the group of 5 prosumers relative to their self-sufficiency. This discrepancy could indicate potential transmission issues (e.g. over-voltage) due to network constraints. In comparison to DSO A and B, DSO C has a relatively low PV penetration level (at 3.8%), with no recorded losses due to temporal and/or spatial mismatch between their production and consumption ($\%PV_{prod/cons} = \%PV_{self\text{-}sufficiency}$). In addition, the wider range of available network levels (NE 2–7), would provide more control over diverting production surpluses to balance supply and demand within this particular network area.

3.2. Critical times and potential flexibility options visualized across day/week/year

Here we assess when flexibility needs are most critical by combining visualization techniques with daily flexibility indicators. This approach reveals how changing production/consumption patterns (daily/weekly/seasonal) directly impact flexibility needs throughout the year. In addition to identifying critical times, the patterns can also reveal potential flexibility options that may be available to address them.

In Fig. 3, DSO B time series profiles of consumption, PV production, and net flow of electricity (across the system boundary) are represented as heatmaps for the full year, while their impact on daily PV utilization and net load variability is shown in the sideplots. In the top row, plotting consumption magnitudes at each timestep ($P(t)$) reveals the presence of regularly scheduled loads during the day, a distinct weekday–weekend demand pattern (i.e. drop in consumption during weekends and weekday holidays), as well as noticeably higher consumption during the colder months (Jan–March, Nov–Dec). With respect to PV production, intra- and inter-day variability (due to weather changes), as well as its seasonally-dependent availability (due to the duration of day-lighting hours) and intensity (due to solar elevation) is observed. The combined effect of these patterns on PV utilization is summarized in the corresponding sideplot, which compares the daily PV production (from Eq. (2)) to the PV self-sufficiency (from Eq. (4)). While the annual $\%PV_{prod/cons}$ is estimated at 8.7% (see Table 2), the values can range from a few percent in winter to close to 30% in summer. As a result, PV production exceeds PV self-sufficiency ($PV_{prod/cons} > PV_{self\text{-}sufficiency}$) when decreased weekend consumption coincides with increased PV production leading to surpluses, especially in spring/summer.

In the bottom row, plotting the changes in power over the course of a day ($\Delta P(t)$ from Eq. (6)) reveals periodic and seasonally varying patterns, which are correlated with load schedules provided by the DSO, as well as seasonal changes (e.g. sunset/sunrise times). Throughout the year, a number of peaks occur periodically during nighttime hours (approx. between 9pm and 2am local time), associated with DSO-scheduled electric hot water boiler charging times during off-peak hours (black arrows). Other scheduled loads for this DSO include switch-off times of direct electric heaters and heat pumps (observed as a reductions in load) occurring around 8am and 11:30am (blue arrows), which have a largest effect in the colder months of the year (also observed as a seasonally-dependent increase in load following the 1-hr shut-off). The observed load reduction following a peak at noon (gray arrow) has not been identified as a scheduled load; however, it may be associated with lunchtime loads of heating (e.g. office kitchen microwaves [40]) and/or preparing food (e.g. workplace canteens). Another seasonally-varying load, which increases at sunset (yellow arrow) is indicative of indoor/outdoor lighting loads. Daily PV production changes follow a general bell-curve shape from sunrise to sunset. However, sudden and frequent fluctuations in PV production occur during most of the year, which are also reflected in the observed variability in net electricity flow. This effect is summarized in the corresponding sideplot by comparing the daily load variability (as defined in Eq. (7)) of net electricity flow (orange) and consumption (gray); the difference between the two indicates the additional variability arising from weather-dependent PV production.

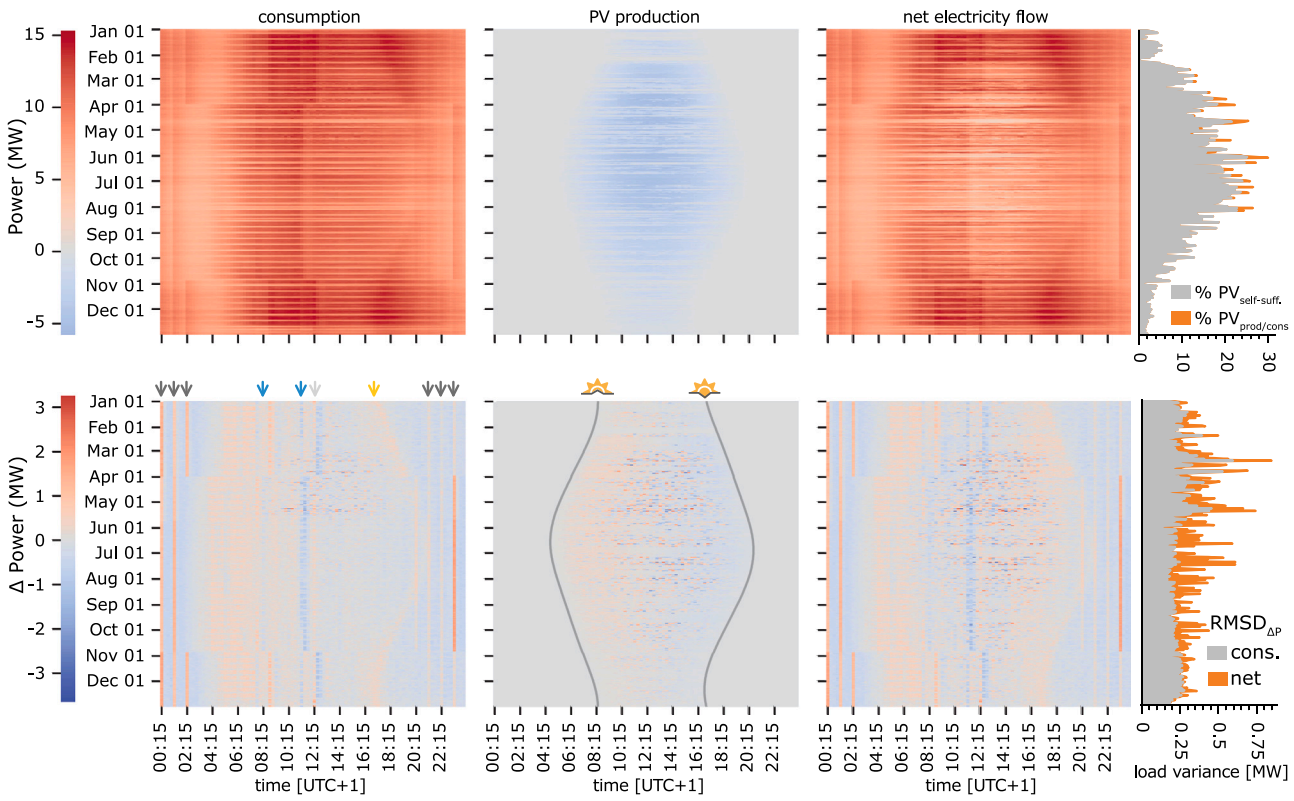

Fig. 3. Load visualization across day and year for DSO B using heatmaps to show their intra-daily/weekly/seasonal patterns, including their impact on PV utilization and net load variability throughout the year (sideplots). The 15-min load profiles, and the corresponding changes in load, are shown in the top and bottom rows, respectively. Periodic and seasonally-varying patterns, which they reveal (indicated by the arrows), are explained in the main text. The impact of seasonal variability on PV production and self-sufficiency, as well as increased intra-daily load variability, are shown in the top and bottom sideplots, respectively.

In Fig. 4, we compare consumption patterns between the three different DSOs throughout the year. In the top row, we plot their changes in demand throughout the day (ΔP) over the course of the year. We observe presence of scheduled loads; some of them are relatively constant throughout the year (e.g. electric boilers), while others seasonally-dependent (e.g. heat pumps and direct electric heating). While the scheduling times and the types of loads are specific to a particular DSO, the three investigated here also appear to share certain commonalities: a ramp-up in load in the early morning hours, a peak followed by a drop around noon, and a second ramp-up in load around sunset, which appears most prominent during winter. Following this peak, the loads generally decrease into the late night/early morning hours.

Below each heatmap, the average daily consumption and production patterns are shown for four months representative of each season; weekday and weekend demand are shown separately in blue and (dashed) gray, respectively, with the corresponding PV production shown in orange. With respect to demand, we observe seasonal dependence in both the magnitude and the shape of the profiles, especially during daytime hours. We observe that the overall demand is highest in winter and lowest in summer for all three DSOs. Additionally, the presence of the late afternoon (sunset) peak is most prominent in winter and fall when day-lighting hours are short. The overall higher daytime winter demand appears dominated by electrified heating, while the late afternoon peak by the longer duration of indoor lighting demand during waking hours in winter in addition to the mostly constant outdoor lighting between sunset and sunrise. For all three DSOs, we also observe a reduced weekend demand, including a more gradual ramp-up in the morning hours, and a (first) peak around mid-day. The relative magnitudes between the weekday and weekend demand can be attributed to relative portions of the type and relative intensities of different economic sectors served by the DSOs compared to their residential demand, which was not investigated here.

When compared to the observed demand patterns, seasonality in PV demand, with regards to its shape and intensity shows that (1) the mismatch between PV production and demand is highest during winter weekdays and lowest during summer weekends and (2) peak PV production lags the mid-day peak demand (more prominent in spring/summer due to the solar noon occurring later in the day—1 hr shift forward in local time). With regards to the general daily trends between production and consumption, daytime demand during summer and spring weekdays appear to match most closely. During winter and fall, the more prominent afternoon peak starts ramping up around sundown, and, consequently, is expected to contribute significantly to the unmet demand. With regards to variability, while the average PV production follows a “bell curve” shape (from sunset to sunrise) throughout the year, we showed that, during this time, production levels can still drop to negligible levels during most of the year, as well as have frequent and/or steep fluctuations, most notably during spring months (as shown in Fig. 3).

The observed demand patterns also give clues about the potential flexibility options that can be used to shift end-consumer demand and improve utilization of PV electricity – namely electricity-based DHW boilers and SH – as they appear as scheduled and seasonal loads, respectively. Both have a heat storage ability, which can provide a good flexibility measure. The scheduled DHW loads identified in the heatmaps, are also observed in the average daily profiles. However, seasonal changes in electric consumption are attributed to a combination of heating demand (throughout the day), lighting demand (starting at sundown), and lifestyle changes (in the evening hours) during both weekdays and weekend, which would require further processing to adequately estimate their individual contributions.

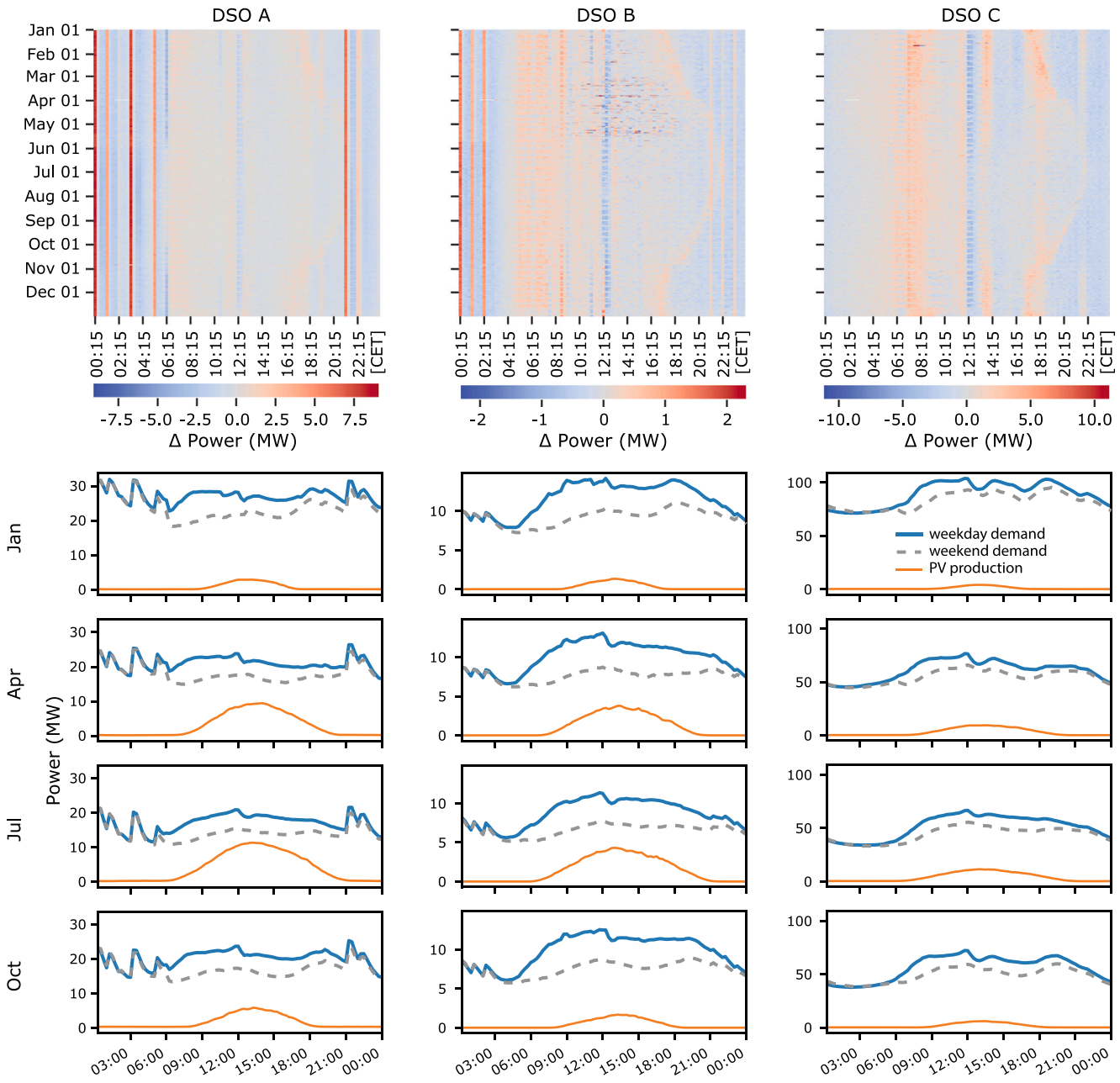

Fig. 4. Consumption patterns over the year represented as heatmaps for each DSO. Average daily consumption profiles for weekdays (blue lines) and weekends (dashed gray lines), with corresponding average PV production (orange lines), during the months representative of each season.

3.3. Potential benefits and limits of intra-daily load-shifting on PV utilization

In Figs. 5 and 6, we explore the impacts of increased PV production on energy flexibility requirements at different timescales within and between DSOs, respectively. In Fig. 5 we compare three entities (from left to right): (1) a group of five prosumers, (2) the feed-in from an upstream transformer station, and (3) the full balancing area of DSO A. For each PV production level (x-axis), annual PV self-sufficiency (y-axis) is computed for the base case (gray sections), as well as when energy flexibility requirements are met at different timescales (colored bar sections). For the given consumption/production profiles, the latter provides the best case scenarios for each timescale assuming an ideal VESS. Horizontal lines mark the maximum attainable annual PV self-sufficiency at each level (i.e. 100% PV self-consumption). In addition to the annual, daily PV self-sufficiency is shown for the 40% case, where hatched areas indicate excess PV production (after energy flexibility requirements are met). In all cases, largest benefit for increased PV self-sufficiency are realized at the 6–12-hr timescale, as mid-day production surpluses are shifted to meet night-time demand. The following flexibility window (12–24 hrs), provides a comparatively smaller additional benefit over the full year, most likely due to high variability at these timescales occurring during times of the year with lower overall production and shorter days (e.g. fall, spring). Due to differences in weekday/weekend demand patterns (as shown in Fig. 4), we would expect there to be a need for a 3-day flexibility. Nevertheless, reaching maximum annual self-sufficiency would require seasonal storage, with summer surpluses shifted to meet winter demand.

The match between PV production and demand appears highest for the entire service area of DSO A. Considering the 40% PV production case, DSO A is able to achieve approx. 30% annual PV self-sufficiency for the base case, approaching the maximum 40% when energy flexibility requirements are met. On the other hand, the group of prosumers,

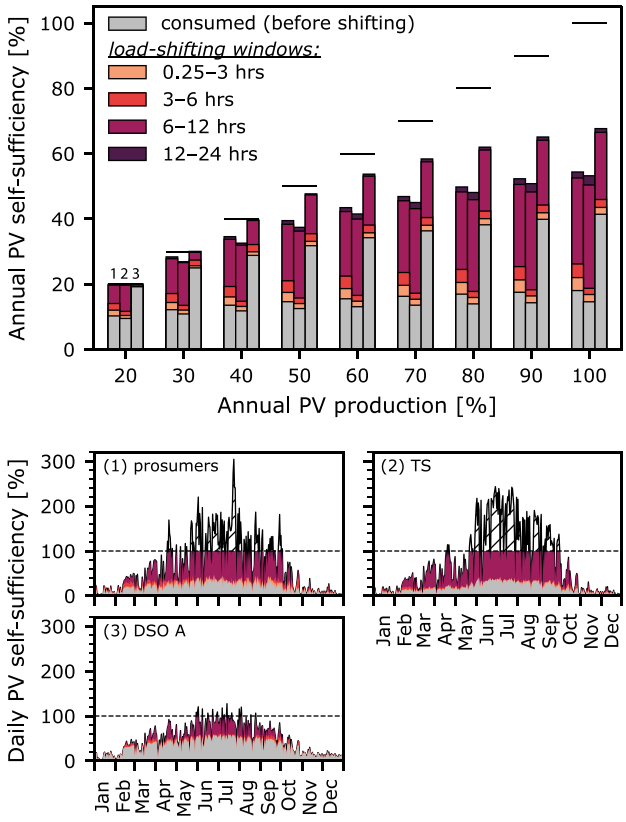

Fig. 5. Estimated impact of daily and seasonal production and consumption patterns on PV utilization and energy flexibility requirements for (1) a group of five prosumers, (2) the feed-in from an upstream transformer station, and (3) the full balancing area of DSO A. Annual PV self-sufficiency (y-axis) at each PV production level (x-axis) for the base case (gray) and when energy flexibility requirements are met at different timescales (colors). Horizontal lines mark the maximum attainable PV self-sufficiency (i.e. 100% PV self-consumption); the difference is the unused PV production (shown as hatched areas in the graphs below). At the 40% annual production, daily PV self-sufficiency throughout the year is plotted for each indicated group.

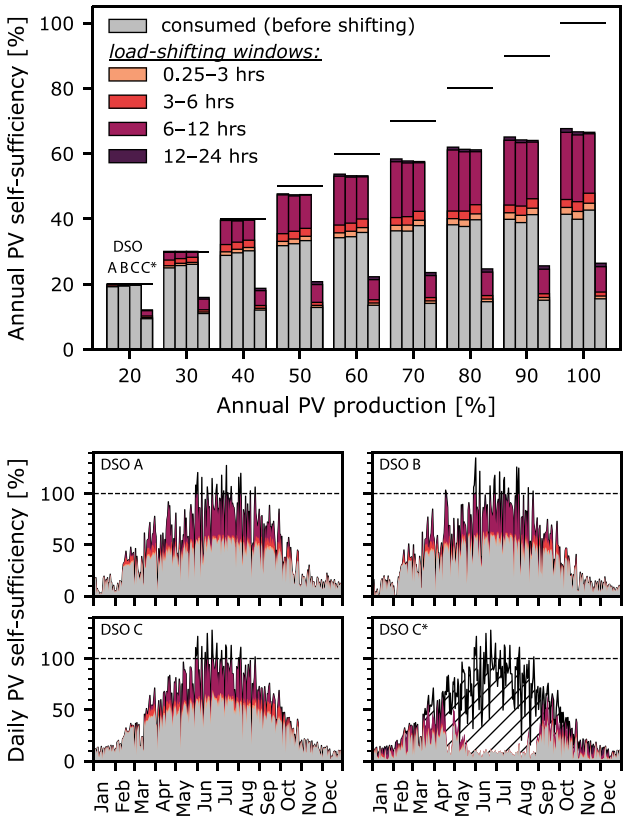

Fig. 6. Annual PV self-sufficiency (y-axis) at each PV production level (x-axis) without load shifting (gray) and when energy flexibility requirements are met at different timescales (colors). Horizontal lines mark the maximum PV self-sufficiency (100% PV self-consumption); the difference is the unused PV production (shown as hatched areas for the graphs below). At the 40% annual production, daily PV self-sufficiency throughout the year is plotted for each DSO, with DSO C shown for cases without and with current hydroelectricity (C and C*, respectively).

together with the surrounding residential area supplied by the transformer station, are only able to directly meet about 10% of their demand without energy flexibility. Even if all intra-daily energy flexibility requirements can be met, they still fall significantly below the maximum PV self-sufficiency at the 40% annual PV production. Their lower PV utilization compared to the full DSO appears related to their differences in typical daily demand profiles—higher daytime demand of the full DSO area provides a better match to PV production profiles. For instance, PV utilization during winter is approaching its maximum without load shifting, and smaller volumes need to be shifted within the day in the period from spring to fall. On the other hand, for both the prosumers and the TS, intra-daily load-shifting appears needed even in winter, and higher shares of load require shifting during the rest of the year. Their production surpluses are also significant during summer months compared to the full DSO area for the same annual PV adoption level. From the prosumer survey responses and their profiles, 3 out of 5 use heat pumps as their main source for space heating. Their significantly higher winter loads dominate their annual demand when compared to the full DSO area. As a result, seasonal storage needs that optimize PV self-consumption are higher for this group compared to the full DSO area.

The presented comparison of PV utilization for both the local (prosumer/TS) and aggregated (DSO A) PV production and demand further illustrates the heterogeneity in flexibility needs within the DSOs, which primarily arise due to their differences in demand patterns. With reduced spatial (i.e network) inter-connectivity, as is the case in DSO A, spatial imbalances within the DSO can lead to an overall reduction in PV utilization for the DSO area (see Table 2).

Similarly, in Fig. 6, we compare PV utilization of the three DSOs. For DSO C, two cases are shown – without and with current hydroelectric generation – indicated as C and C*, respectively. Despite existing differences in their demand patterns (see Fig. 4), their estimated annual PV self-sufficiency values all lie within a narrow range; negligible differences are observed for the 20% PV production case, reaching 3% for the net-zero (i.e. 100% PV production) case. With the assumption that loads can be spatially shifted within the DSO network area, an annual PV self-sufficiency approaching 20% appears achievable for the base case (with negligible surplus production). At 40%, ideal intra-daily load-shifting leads to maximum benefits with negligible outflows (nearly 100% PV self-consumption), where the 6–12 hr load-shifting window provides the largest share. The accompanying daily PV self-sufficiency graphs (excluding DSO C*), show that surplus production occurs in the limited case during summer weekends (Jun–Aug). The annual PV self-sufficiency shows a saturation trend in the range 70%–100% for all the three cases. In this range, a VESS operating on the intra-daily timescale is unable to utilize the surpluses in summer, while still experiencing high deficits in winter, requiring the need for seasonal storage.

For the case when non-PV generation is included for DSO C (depicted in the figure as DSO C*), which is primarily supplied with hydro power, the utilization of PV electricity within the DSO is expected to be either (1) limited to the times when hydroelectric generation is unable to meet the demand for the DSO (as shown in the figure), or (2) hydroelectric generation would need to reduce its supply of energy

volume within the DSO to complement increased PV production. Due to the seasonality of hydro production, similar to that of PV production – highest in summer and lowest in winter – PV production would provide least benefit between May and August when both hydroelectric and PV production are at their highest levels.

3.4. Limitations and further work

The presented approach for evaluating energy flexibility is currently limited to intra-daily flexibility (up to 24 hrs) due to its relevance for demand-side management and battery storage. The flexibility requirements of a VESS between 24 hrs and seasonal is briefly discussed, and will be a focus of future work. Additionally, due to the simplicity of the model, which uses aggregated time series profiles, the presence of spatial mismatch within the DSO boundary can only be evaluated for the present state (using the above-mentioned VRE utilization indicators). For the future projections, flexibility needs are based solely on the temporal mismatch within the DSO boundary. However, based on the current state, one can decide whether a more detailed model may be needed to evaluate potential solutions that address spatial mismatch in the region (e.g. grid expansion).

The impact of temporal resolution on the results has not been investigated in this study. Nevertheless, as pointed out by other studies [41–43] there can be significant differences in the results when using hourly and sub-hourly resolution, especially in estimating the overall surpluses and deficits that arise due to the temporal mismatch between production and consumption. Specifically, temporal resolution limits the ability to capture the temporal mismatch that may be occurring below the temporal resolution of the analyzed data, which becomes a concern at high spatial resolution where generation and demand profiles are more stochastic [43].

In addition, while our analysis is specific to the three DSOs presented here (serving small to medium towns in Switzerland), the general trends we observed, driven by diurnal and seasonal cycles of solar production, are expected to hold true for other regions with similar daily and seasonal demand patterns (e.g. heating as the main seasonal driver of electricity use). Nevertheless, the presented methodology can be readily applied to areas with significantly different VRE generation (e.g. wind), latitude position, weather conditions (e.g. cloud coverage), as well as load patterns (e.g. cooling as a dominant seasonal load) in order to gain regionally-specific insights. At the same time, while measured data may not be available in many cases, the presented approach for estimating energy flexibility needs could be applied to fully modeled data, and/or a combination of measured, modeled and projected loads and generation patterns. Further analysis would also be helpful to understand how changes in load shape due to a number of factors – such as electrification of mobility and space heating, as well as the impacts of climate change on heating and cooling loads – impact the results.

Lastly, while we have identified two main sources of flexibility based on the consumption patterns of the DSOs – space heating and domestic hot water – future studies could quantify the energy flexibility that these sources would be able to provide in each of the regions considered, in addition to including the emerging sources of flexibility (e.g. electricity-based mobility).

4. Conclusion

Using existing load profiles from distribution system operators (DSOs), the study set out to develop a generalized, scalable method to estimate regional utilization of variable renewable energy (VRE), as well as corresponding energy flexibility requirements at different timescales, for both current and scaled-up VRE penetration levels. Based on a case study of three small- to medium-sized DSOs in Switzerland, we provide the following key takeaways:

- With regards to energy flexibility needs (in the context of VRE utilization), we have shown that utilities with similar photovoltaic (PV) production levels can significantly vary in their ability to consume the produced electricity within their network areas, despite having comparable demand patterns. The observed discrepancies in PV self-consumption appear mainly influenced by their respective network topologies; comparison of their *net* and *actual* PV self-sufficiency indicators revealed differences in their ability to displace localized PV production surpluses to other areas within their network boundary. If only temporal mismatch is considered, their comparable demand patterns lead to minor differences in the future energy flexibility requirements (within 3%), where the PV penetration level is the most influential factor (in the absence of other generation sources).
- When PV production and demand are aggregated – from the individual prosumer to a group – higher portion of PV-generated electricity is self-consumed due to variations in both supply and demand profiles, thereby reducing the energy flexibility requirements.
- For the DSO having hydroelectric power as the main source of production, we have shown that the seasonality of hydro production (highest in summer, lowest in winter) may either limit PV utilization in summer or reduce the reliance on hydroelectricity to meet summer demand.
- Critical times arise at different timescales – across day/week/year – due to the changing production and consumption patterns. DSOs experience highest deficits during winter weekdays, and highest surpluses during summer weekends. Additionally, PV production levels can drop to negligible levels during most of the year, as well as experience frequent and/or steep fluctuations, especially during spring months.
- Assuming that a virtual energy storage system (VESS) can meet the estimated intra-daily energy flexibility requirements, we showed that (1) ~40% of energy demand could be met with PV production while minimizing production surpluses (i.e nearly 100% PV self-consumption) and (2) the largest gains in PV utilization could be achieved at the 6–12 hr timescale, which address the diurnal PV production cycle (especially from spring to fall). For PV production levels beyond 70% of annual consumption, we observe a saturation trend. In this range, additional gains in PV self-sufficiency are limited by the seasonal PV production cycle, where small gains in winter coincide with high surpluses in summer.

The results of the case study demonstrate the importance of accounting for regional differences in the assessment of VRE utilization and energy flexibility requirements. The presented approach, based on aggregated profiles at the local (DSO) level in combination with the proposed indicators, could be readily applied to different areas for initial evaluation. Their results could serve as a basis for determining regionally-specific challenges to VRE integration, as well as a suitable mix of technological and market-based strategies needed to address them.

CRediT authorship contribution statement

Natasa Vulic: Conceptualization, Methodology, Formal analysis, Data curation, Visualization, Writing – original draft. **Martin Rüdisüli:** Supervision, Project administration, Writing – review & editing. **Kristina Orehounig:** Supervision, Funding acquisition, Writing – review & editing.

Declaration of competing interest

The authors declare that they have no known competing financial interests or personal relationships that could have appeared to influence the work reported in this paper.

Data availability

The authors do not have permission to share data.

Acknowledgments

The project was funded by the Swiss Federal Office of Energy (Section: Energy Research and Cleantech) under the project titled "aliunid - Versorgung 'neu': Feldtest 1.1.2019 – 30.6.2020" (SI/501841). Sinan Teske is acknowledged for his preliminary work with setting up the project. The authors would also like to thank the DSOs and the company aliunid for providing the raw data and additional information.

References

[1] World Energy Council. World energy trilemma index. 2016, URL https://www.worldenergy.org/assets/downloads/Executive-summary_Energy-Trilemma-Index-2016.pdf.
[2] IEA. Global energy review 2020: The impacts of the Covid-19 crisis on global energy demand and CO2 emissions. Tech. rep., International Energy Agency; 2020.
[3] IRENA. Renewable capacity statistics 2020. Tech. rep., International Renewable Energy Agency (IRENA); 2020, URL https://www.irena.org/publications/2020/Mar/Renewable-Capacity-Statistics-2020.
[4] IEA. Global energy review 2019: The latest trends in energy and emissions in 2019. Tech. rep., International Energy Agency; 2020.
[5] Langevin J, Harris CB, Satre-Meloy A, Chandra-Putra H, Speake A, Present E, et al. US building energy efficiency and flexibility as an electric grid resource. Joule 2021;5(8):2102–28. http://dx.doi.org/10.1016/j.joule.2021.06.002.
[6] Li H, Wang Z, Hong T, Piette MA. Energy flexibility of residential buildings: A systematic review of characterization and quantification methods and applications. Adv Appl Energy 2021;3:100054. http://dx.doi.org/10.1016/j.adapen.2021.100054.
[7] Sun Q, Li H, Ma Z, Wang C, Campillo J, Zhang Q, et al. A comprehensive review of smart energy meters in intelligent energy networks. IEEE Internet Things J 2016;3(4):464–79. http://dx.doi.org/10.1109/JIOT.2015.2512325.
[8] Strbac G. Demand side management: Benefits and challenges. Energy Policy 2008;36(12):4419–26. http://dx.doi.org/10.1016/j.enpol.2008.09.030.
[9] Bloess A, Schill W-P, Zerrahn A. Power-to-heat for renewable energy integration: A review of technologies, modeling approaches, and flexibility potentials. Appl Energy 2018;212:1611–26. http://dx.doi.org/10.1016/j.apenergy.2017.12.073.
[10] Bibak B, Tekiner-Moğulkoç H. A comprehensive analysis of vehicle to grid (V2G) systems and scholarly literature on the application of such systems. Renew Energy Focus 2021;36:1–20. http://dx.doi.org/10.1016/j.ref.2020.10.001.
[11] Daiyan R, MacGill I, Amal R. Opportunities and challenges for renewable power-to-x. ACS Energy Lett 2020;5(12):3843–7. http://dx.doi.org/10.1021/acsenergylett.0c02249.
[12] Pudjianto D, Ramsay C, Strbac G. Virtual power plant and system integration of distributed energy resources. IET Renew Power Gener 2007;1(1):10–6. http://dx.doi.org/10.1049/iet-rpg:20060023.
[13] Eid C, Codani P, Perez Y, Reneses J, Hakvoort R. Managing electric flexibility from distributed energy resources: A review of incentives for market design. Renew Sustain Energy Rev 2016;64:237–47. http://dx.doi.org/10.1016/j.rser.2016.06.008.
[14] Cheng M, Sami SS, Wu J. Benefits of using virtual energy storage system for power system frequency response. Appl Energy 2017;194:376–85. http://dx.doi.org/10.1016/j.apenergy.2016.06.113.
[15] SWECO. Study on the effective integration of distributed energy resources for providing flexibility to the electricity system. Tech. rep., European Commision; 2015.
[16] IRENA. Innovations landscape brief: future role of distribution system operators. Tech. rep., International Renewable Energy Agency (IRENA); 2019, URL https://www.irena.org/-/media/Files/IRENA/Agency/Publication/2019/Feb/IRENA_Landscape_Future_DSOs_2019.pdf?la=en&hash=EDEBEDD537DE4ED1D716F4342F2D55D890EA5B9A.
[17] Prettico G, Flammini M, Andreadou N, Vitiello S, Fulli G, Masera M. Distribution system operators observatory 2018: overview of the electricity distribution system in Europe. Publications Office of the European Union; 2019, http://dx.doi.org/10.2760/104777.
[18] Kufeoglu S, Pollitt M, Anaya K. Electric power distribution in the world: Today and tomorrow. In: Cambridge working papers in economics. Faculty Apollo - University of Economics Cambridge Repository; 2018, p. na–na. http://dx.doi.org/10.17863/CAM.27667.
[19] Mateo C, Prettico G, Gómez T, Cossent R, Gangale F, Frías P, et al. European representative electricity distribution networks. Int J Electr Power Energy Syst 2018;99:273–80. http://dx.doi.org/10.1016/j.ijepes.2018.01.027.
[20] Coster EJ, Myrzik JM, Kruimer B, Kling WL. Integration issues of distributed generation in distribution grids. Proc IEEE 2010;99(1):28–39. http://dx.doi.org/10.1109/jproc.2010.2052776.
[21] Walling R, Saint R, Dugan RC, Burke J, Kojovic LA. Summary of distributed resources impact on power delivery systems. IEEE Trans Power Deliv 2008;23(3):1636–44. http://dx.doi.org/10.1109/tpwrd.2007.909115.
[22] Fuchs A, Demiray T. Large-scale PV integration strategies in distribution grids. In: 2015 IEEE Eindhoven Powertech. 2015, p. 1–6. http://dx.doi.org/10.1109/PTC.2015.7232811.
[23] Perera A, Nik VM, Wickramasinghe P, Scartezzini J-L. Redefining energy system flexibility for distributed energy system design. Appl Energy 2019;253:113572. http://dx.doi.org/10.1016/j.apenergy.2019.113572, URL https://www.sciencedirect.com/science/article/pii/S0306261919312462.
[24] Koivisto M, Das K, Guo F, Sørensen P, Nuño E, Cutululis N, et al. Using time series simulation tools for assessing the effects of variable renewable energy generation on power and energy systems. Wiley Interdisc Rev Energy Environ 2018;8(3):e329. http://dx.doi.org/10.1002/wene.329.
[25] Ueckerdt F, Brecha R, Luderer G, Sullivan P, Schmid E, Bauer N, et al. Representing power sector variability and the integration of variable renewables in long-term energy-economy models using residual load duration curves. Energy 2015;90:1799–814. http://dx.doi.org/10.1016/j.energy.2015.07.006, URL https://www.sciencedirect.com/science/article/pii/S0360544215008993.
[26] Lannoye E, Flynn D, O'Malley M. Evaluation of power system flexibility. IEEE Trans Power Syst 2012;27(2):922–31. http://dx.doi.org/10.1109/tpwrs.2011.2177280.
[27] Heggarty T, Bourmaud J-Y, Girard R, Kariniotakis G. Multi-temporal assessment of power system flexibility requirement. Appl Energy 2019;238:1327–36. http://dx.doi.org/10.1016/j.apenergy.2019.01.198.
[28] Denholm P, Mai T. Timescales of energy storage needed for reducing renewable energy curtailment. Renew Energy 2019;130:388–99. http://dx.doi.org/10.1016/j.renene.2018.06.079.
[29] Olsen KP, Zong Y, You S, Bindner H, Koivisto M, Gea-Bermúdez J. Multi-timescale data-driven method identifying flexibility requirements for scenarios with high penetration of renewables. Appl Energy 2020;264:114702. http://dx.doi.org/10.1016/j.apenergy.2020.114702.
[30] Holttinen H, Kiviluoma J, Estanqueiro A, Aigner T, Wan Y-H, Milligan MR. Variability of load and net load in case of large scale distributed wind power. In: 10th international workshop on large-scale integration of wind power into power systems as well as on transmission networks for offshore wind power farms. 2010, p. na–na, arXiv:http://hdl.handle.net/10197/4722.
[31] Denholm P, Hand M. Grid flexibility and storage required to achieve very high penetration of variable renewable electricity. Energy Policy 2011;39(3):1817–30. http://dx.doi.org/10.1016/j.enpol.2011.01.019.
[32] Swisssolar. Photovoltaik. 2019, URL https://www.swissolar.ch/ueber-solarenergie/photovoltaik/.
[33] Pronovo. Einspeisevergütungssystem (EVS) Mehrkostenfinanzierung (MKF). Jahresbericht, Pronovo AG; 2019.
[34] Kirchner A, Bredow D, Ess F, Grebel T, Hofer P, Kemmler A, et al. Die Energieperspektiven für die Schweiz bis 2050. Bundesamt für Energie (BFE) 2012.
[35] Axpo. The Swiss electricity market. 2018, URL https://www.axpo.com/ch/en/about-us/media-and-politics/power-market-switzerland.html.
[36] Swiss Federal Office of Energy: Energy Research and Cleantech. Aliunid - Versorgung "neu": Feldtest 1.1.2019–30.6.2020 (SI/501841). 2020, URL https://www.aramis.admin.ch/Texte/?ProjectID=43459.
[37] Swissgrid. Grid levels, URL https://www.swissgrid.ch/en/home/operation/power-grid/grid-levels.html.
[38] Luthander R, Widén J, Nilsson D, Palm J. Photovoltaic self-consumption in buildings: A review. Appl Energy 2015;142:80–94. http://dx.doi.org/10.1016/j.apenergy.2014.12.028.
[39] Yarbrough I, Sun Q, Reeves D, Hackman K, Bennett R, Henshel D. Visualizing building energy demand for building peak energy analysis. Energy Build 2015;91:10–5. http://dx.doi.org/10.1016/j.enbuild.2014.11.052.
[40] Menezes A, Cripps A, Buswell R, Wright J, Bouchlaghem D. Estimating the energy consumption and power demand of small power equipment in office buildings. Energy Build 2014;75:199–209. http://dx.doi.org/10.1016/j.enbuild.2014.02.011.
[41] Wright A, Firth S. The nature of domestic electricity-loads and effects of time averaging on statistics and on-site generation calculations. Appl Energy 2007;84(4):389–403. http://dx.doi.org/10.1016/j.apenergy.2006.09.008, URL https://www.sciencedirect.com/science/article/pii/S0306261906001097.
[42] Cao S, Sirén K. Impact of simulation time-resolution on the matching of PV production and household electric demand. Appl Energy 2014;128:192–208. http://dx.doi.org/10.1016/j.apenergy.2014.04.075, URL https://www.sciencedirect.com/science/article/pii/S0306261914004383.
[43] Tumminia G, Guarino F, Longo S, Aloisio D, Cellura S, Sergi F, et al. Grid interaction and environmental impact of a net zero energy building. Energy Convers Manage 2020;203:112228. http://dx.doi.org/10.1016/j.enconman.2019.112228, URL https://www.sciencedirect.com/science/article/pii/S0196890419312348.